Desalination and Water Treatment
www.deswater.com

doi: 10.1080/19443994.2014.944220

56 (2015) 1309–1320
October

Taylor & Francis
Taylor & Francis Group

Evaluating the performance of PEG-based scale inhibition and dispersion agent in cooling water systems

Yahui Liu[a], Yuming Zhou[a,b,*], Qingzhao Yao[a,b,*], Wei Sun[c]

[a]*School of Chemistry and Chemical Engineering, Southeast University, Nanjing 211189, P.R. China, Tel. +86 25 52090617; emails: liuyahui0925@126.com (Y. Liu), ymzhou@seu.edu.cn (Y. Zhou), 101006377@seu.edu.cn (Q. Yao)*
[b]*Jiangsu Optoelectronic Functional Materials and Engineering Laboratory, Nanjing 211189, P.R. China*
[c]*Jianghai Environmental Protection Co. Ltd, Changzhou 213116, Jiangsu, P.R. China, Tel. +86 25 52090617; email: 1643792504@qq.com*

Received 13 November 2013; Accepted 7 July 2014

ABSTRACT

In this paper, a new double hydrophilic and environment-friendly polyether copolymer inhibitor, polyethylene glycol double-ester of maleic anhydride—acrylic acid (PEGDMA-AA), was synthesized to inhibit the precipitation of calcium carbonate and Fe(III) scales. Structures of PEG, PEGDMA, and PEGDMA-AA were characterized by Fourier transform infrared spectrometer (FTIR) and ^{1}H Nuclear Magnetic Resonance (^{1}HNMR). The influence of PEGDMA-AA dosage and mass ratio (PEGDMA: AA) toward $CaCO_3$ and Fe scale were tested through static jar scale inhibition and dispersion tests. The optimal mass ratio (PEGDMA: AA) was 1:1 for calcium carbonate inhibition and 1:2 for dispersing Fe(III), respectively. Investigation of influence of solution properties on $CaCO_3$ inhibition was also carried out and dispersion ability for Fe(III) was compared with commercial inhibitors. The effect of PEGDMA-AA on the morphology, size, and crystal form of $CaCO_3$ particles were examined through scanning electron microscopic, transmission electron microscope, X-ray powder diffraction, and FTIR. One supposed mechanism (core–shell structure) was also described in detail.

Keywords: Double-hydrophilic; Calcium carbonate; Ferric scale; PEG; Core-shell

1. Introduction

The need for great amount of water in industrial fields is increasing sharply. Limited by the lack of water resources and to cut down the consumption, the once-through cooling water system has been replaced by the recycling circulate water system [1–6]. And in this case severe phenomena of corrosion, scale precipitation, and microbial propagation took place undesirably, bringing about technical and economical problems such as decreased system heat transfer efficiency and increased cleaning frequency even unexpected system shutdowns [7,8]. Caused by the motivation to settle the problems, addition of effective inhibitors consisting of strong complexation functional groups, also with superior dispersion characteristic are commonly used in the water system, including the polycarboxylate and polyphosphate antiscalants, such as PAA, HPMA, PBTC, PAPEMP, ATMP, HEDP [9–12]. However, the performance of retarding scale formation and deposition is not something delightful.

*Corresponding authors.

Polycarboxylate inhibitors may form insoluble calcium-polymer salts due to its low calcium tolerance [13,14] and can exist for a certain period after emission, while the polyphosphate hydrolysis in water to produce orthophosphate and form insoluble calcium phosphate depositions with positive ions. Except for the above-mentioned unfavorable disadvantages, inhibitors which are made up of phosphorous element gives rise to the water eutrophication after discharged, which is also a great concern and challenge to environment protection [15]. So phosphonates should be limited to be used in water treatment.

Among all scales, calcium carbonate scale is the most frequently generated scale in heat transfer surface [8,16] depending on the saturation of the water conditions. Temperature, pH, evaporation of the solution, dissolved gases, microorganisms, algae, etc. are all the indeterminacy term affecting the formation of super-saturation degree thus accelerating or retarding the crystallization of scales [17]. Calcite, aragonite, and vaterite are the typical three forms of calcium carbonate [18,19]. Among the three crystal forms, less stable aragonite and vaterite can transform into the greatest thermodynamically calcite spontaneously, but in the presence of inhibitors, the phase transformation process to calcite is prohibited [12,19,20]. Plummer and Busenberg studied the relation between the solubility of $CaCO_3$ and temperature which is to be negative correlation. In other words, the higher temperature is advantageous to the deposition occurrence of $CaCO_3$ scale. Generally, acid picking is the mostly used method to slacken the scale layer and then wash away scales out by the flowing line [18]. But this method can lead to metal tube corrosion, so design and use of chelating chemicals and threshold inhibitors is becoming more and more dominating [21]. The mechanism of the behavior on the scale is attributed to the formation of soluble complex after chelating between positive ions and high polymers, in which carboxylate anions play the role of binding sites related to the binding energy [17,22]. Another mechanism is the absorption on the surface of scale deposition, interfering or violating the growth tendency and crystalline, so as to alter and change the morphology, pattern, and size of the scales [23,24].

Iron-based compounds such as ferric chloride and ferric sulfate in feed waters are the main sources of iron in cooling towers [25]. Other sources of iron include boiler condensate, corrosion products from pumps and pipes, and biological activity (transformation of iron during bacterial processes) [26]. When the valence state is lower (+2), ferrous iron can dissolve in the solution, which has no severe influence at low pH values of about 3–4, but as pH value increases, problems arise accordingly. Ferrous ions can be oxidized by oxygen gas and other oxidizing agents dissolved or suspended in recycling circulating water. The produced ferric (Fe^{3+}) ions result in the equipment corrosion depositing on heat-exchanger surfaces in three forms of compounds, of which iron hydroxide $Fe(OH)_3$ and iron oxide Fe_2O_3 are the main two forms [7,8,27]. Fe(III) in circulation system can impact the antiscaling performance of inhibitors such as poly acrylic acid (AA) whose role is affected by the formation of insoluble iron phosphate deposit. Meanwhile, fouling brought by iron compounds threatens the efficient operation of industrial recycling water systems [28]. Therefore, control toward the precipitation of compounds consist of ferric such as iron oxide, iron silicates, ferric phosphate and the like is of prime importance to achieve the best performance for water treatment industry. Excellent water treatments should not only have the wonderful inhibition property but also nice dispersion power for Fe(III).

In recent years, double hydrophilic block polymers appeals to be of great interest to polymer researchers for their advantageous structures. Because each block can be designed in an optimum way for the desired use, so different functions are included and separated within one molecule [29]. In this study, a new type of double hydrophilic polyethylene glycol (PEG)-based block polymer for crystal modifier was synthesized whose structure is different with the conventional chelating agents, in which the hydrophilic PEG segments were incorporated whose function is to enhance the water solubility of PEGDMA-AA-Ca^{2+} and PEGDMA-AA-Fe^{3+}, but still being linear polymer. The raw materials used for synthesis are economically efficienct and the polymer is phosphor-free and nitrogen-free. The designed copolymer polyethylene glycol double-ester of maleic anhydride—acrylic acid (PEGDMA-AA) also was first time synthesized in our laboratory.

2. Materials and methods

2.1. Materials and characterization

The PEG used in the experiment was reagent grade and had an average molecular weight of 400. AA, maleic acid (MA), and ammonium persulphate employed were analytically pure grade and supplied by Zhongdong Chemical Reagent Co., Ltd (Nanjing, Jiangsu, P.R. China). Commercial inhibitors of PAA ($M_w = 1{,}800$), HPMA ($M_w = 600$), PESA ($M_w = 1{,}500$), HEDP ($M_w = 206$), and PBTC ($M_w = 270$) were technical grade and supplied by Jiangsu Jianghai Chemical Co., Ltd (Changzhou, Jiangsu, P.R. China). Distilled water was used in all the studies.

Fourier transform infrared (FTIR) spectra were measured on a Bruker FT-IR analyzer (VECTOR-22, Bruker Co., Germany) by using the KBr-pellet method (compressed powder). ^{1}HNMR spectra were recorded on a Mercury VX-500 spectrometer (Bruker AMX500) using tetramethylsilane internal reference and deuterated dimethyl sulfoxide (DMSO-d6) as the solvent. The shapes of calcium carbonate scales were observed with scanning electron microscope (SEM, S-3400 N, HITECH, Japan) and transmission electron microscope (TEM, JEM-2100SX, Japan). The X-ray diffraction (XRD) patterns of the $CaCO_3$ crystals were recorded on a Rigaku D/max 2400 X-ray powder diffractometer with CuKα ($\lambda = 1.5406$) radiation (40 kV, 120 mA). Light transmittance of ferric solutions was measured spectrophotometrically at 420 nm on an ultraviolet-visible 3100-PC spectrometer (Mapada, P.R. China).

2.2. Synthesis of macromonomer of PEGDMA

Transformation into the carboxylate-terminated PEGDMA was performed by the esterification between PEG and maleic anhydride (MA) with the molar ratio 1:2. The yields exceeded 95% and the reaction procedure is shown in Fig. 1.

2.3. Synthesis of PEG-based copolymer PEGDMA-AA

A six-neck round-bottom flask, equipped with a thermometer, a mechanical agitation, and reflux condensing tube was charged with 5 mL deionized water and PEGDMA, and then heated to 80˚C with fierce stirring. Both AA and ammonium persulfate APS were diluted before casting into the reaction unit. Certain amount of AA in 20 mL deionized water and the initiator ammonium persulphate solution in 20 mL deionized water were injected into the flask at constant flow rates over a certain period of 1 and 1.5 h, respectively. After that, temperature was raised to 90˚C and maintained for 2.5 h to finally get the faint yellow liquid with approximately 21% solid content. PEGDMA-AA with different mass ratio was also synthesized. The procedure for the synthesis of PEGDMA-AA was given in Fig. 2.

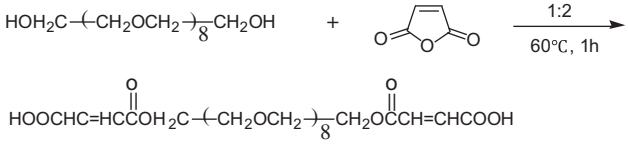

Fig. 1. Synthesis of PEGDMA.

2.4. Static scale inhibition and dispersion test

All deposit experiments were carried out in triplicate and all inhibitor dosage given below were based on a dry inhibitor. Analytical reagent, A grade glassware and deionized water were used throughout. Calcium carbonate scale was deposited by mixing a certain amount of $CaCl_2$ and $NaHCO_3$ solutions according to the national standard of P.R. China, concerning the code for the design of industrial circulating cooling-water treatment (GB/T 16632-2008). The final concentration of Ca^{2+} and HCO_3^- was 240 mg/L and 732 mg/L, respectively, with the solution pH 9 adjusted by borax buffer solution. Investigation with inhibitors and without inhibitors was carried out. Deposition of these calcium carbonate supersaturated solutions were filtered using filter paper after these solutions were incubated at 80˚C for 10 h. The Ca^{2+} ions concentration in the residual filtered fluid was analyzed by EDTA complexometric titration method according to the national standard of P.R. China concerning the code for the design of industrial circulating cooling water treatment (GB/T 15452-2009). At the end point of titration, the color of the solution changed from purple red into dark blue using calcon-carboxylic acid indicator. The copolymer inhibition efficiency for calcium carbonate was calculated with the following equation:

$$\text{Inhibition efficiency}\,(\%) = \frac{[Ca^{2+}]_{final} - [Ca^{2+}]_{blank}}{[Ca^{2+}]_{initial} - [Ca^{2+}]_{blank}} \quad (1)$$

As the equation describes, $[Ca^{2+}]_{final}$ and $[Ca^{2+}]_{blank}$ was the concentration of Ca^{2+} ions in the filtrate liquor in the presence of inhibitor and without the presence of inhibitor after calcium carbonate supersaturated solutions were heated at 80˚C for 10 h. And $[Ca^{2+}]_{initial}$ was the maximum concentration of Ca^{2+} ions at the beginning of the scale tests. Commercial scale inhibitors with different molecular structures and molecular weights such as PAA, HPMA, PBTC, PESA, etc. were also tested to have a inhibition efficiency comparison.

The dispersive capacity test for Fe(III) experiments was carried out by the following procedure. Ferrous sulfate heptahydrate was employed to prepare the fresh ferrous solutions, while the prepared calcium chloride stock solution can be used for a long time. A certain amount of calcium solution was added into a beaker (500 mL) at room temperature with fierce stir. Upon temperature equilibration, different amounts of inhibitors were injected into the beaker just before the addition of fresh ferrous solution. The solution value of pH was adjusted to 9.0 by using borax buffer solution ahead of the addition of Ca^{2+} ions. The final

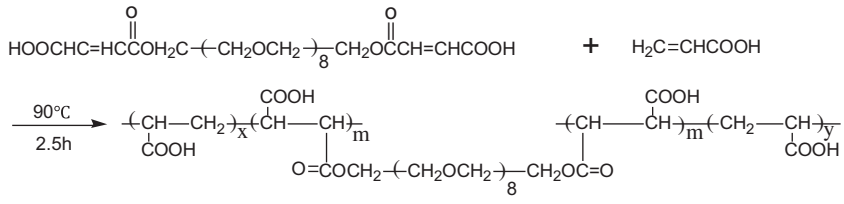

Fig. 2. Synthesis of PEGDMA-AA.

concentration for Ca^{2+} and Fe^{2+} is 150 mg/L and 10 mg/L, respectively. The light transmittance of the artificial solutions was measured by using UV spectrophotometer after heated in thermostat water bath for 6 h at a temperature of 50°C. The lower the light transmittance is, the more excellent the polymer dispersion power is.

3. Result and characterization

3.1. FITR characterization of MA, PEG, PEGDMA, and PEGDMA-AA

The FTIR spectra of MA, PEG, PEGDMA, and PEGDMA-AA are presented in Fig. 3. The strong intensity absorption peak (–C=O) in 1,728 and 1,640 cm^{-1} (–C=C–) in curve c proves that the carboxyl functionalization has happened between PEG and MA, so the PEGDMA is synthesized successfully. No reflection peak for the (–C=C–) stretching vibration appearing at 1,640 cm^{-1} in curve d gives the fact that free radical polymerization underwent between PEGDMA and AA.

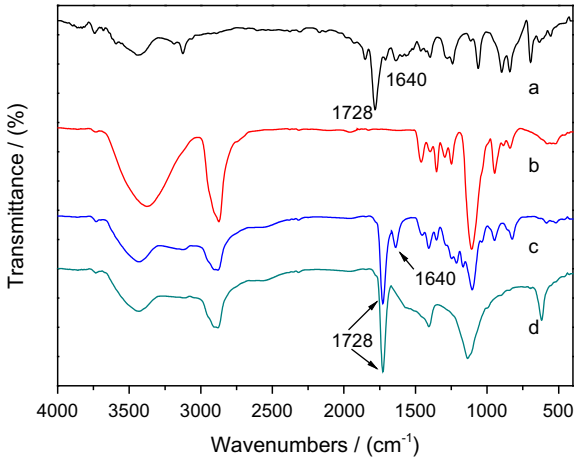

Fig. 3. The FTIR spectra of MA (a), PEG (b), PEGDMA (c), and PEGDMA-AA (d).

3.2. ^{1}HNMR spectra of PEG, PEGDMA, and PEGDMA-AA

The ^{1}HNMR spectra of PEG, PEGDMA, and PEGDMA-AA are presented in Fig. 4.

PEG ($(CD_3)_2SO$, δ ppm): 2.50 (solvent residual peak of $(CD_3)_2SO$), 3.29–3.55 (–OCH_2CH_2–, ether groups), 4.53 (–OH, active hydrogen in PEG) (Fig. 4(a)).

PEGDMA ($(CD_3)_2SO$, δ ppm): 3.48–3.64 (–OCH_2CH_2–, ether groups), 4.19–4.21 (–CH_2OC=O, protons close neighbor to carbonyl group), 6.37 (–CH=CH–, ethylene group) (Fig. 4(b)). It is obvious that hydroxyl group (–OH) δ 4.53 ppm in Fig. 4(a) has disappeared completely and –CH=CH– protons appear in δ 6.37 ppm in Fig. 4(b). Meanwhile, δ 4.20 ppm peaks give the information of the existence of carbonyl group. The above fact suggest that –OH groups in PEG has entirely transformed into –OC(=O)CH=CHCOOH and PEGDMA is synthesized successfully.

PEGDMA–AA ($(CD_3)_2SO$, δ ppm): 2.50 (solvent residual peak of $(CD_3)_2SO$), 3.30–3.51 (–OCH_2CH_2–, ether groups). δ 6.37 ppm double bond adsorption peaks in Fig. 4(b) completely disappears in Fig. 4(c), giving the conclusion that free radical polymerization between PEGDMA and AA has happened.

3.3. Scale inhibition test of $CaCO_3$

3.3.1. Influence of dosage and mass ratio (PEGDMA: AA) on $CaCO_3$ scale inhibition

Fig. 5 presents the relation between inhibitor dosage, mass ratio (PEGDMA: AA), and antiscaling ability towards $CaCO_3$. It is obvious that PEGDMA-AA has a lower calcium tolerance below a certain level of dosage. As the dosage increases gradually, the inhibition efficiency improved substantially and maximum inhibitory power is obtained at a certain dosage named threshold value, except for PEGDMA-AA (mass ratio 2:5). The threshold dosage is 10, 8, 10, and 8 mg/L for PEGDMA-AA (mass ratio 1:2), PEGDMA-AA (mass ratio 1:1), PEGDMA-AA (mass ratio 2:1), and PEGDMA-AA (mass ratio 5:2), respectively, and the corresponding maximum inhibition efficiency is

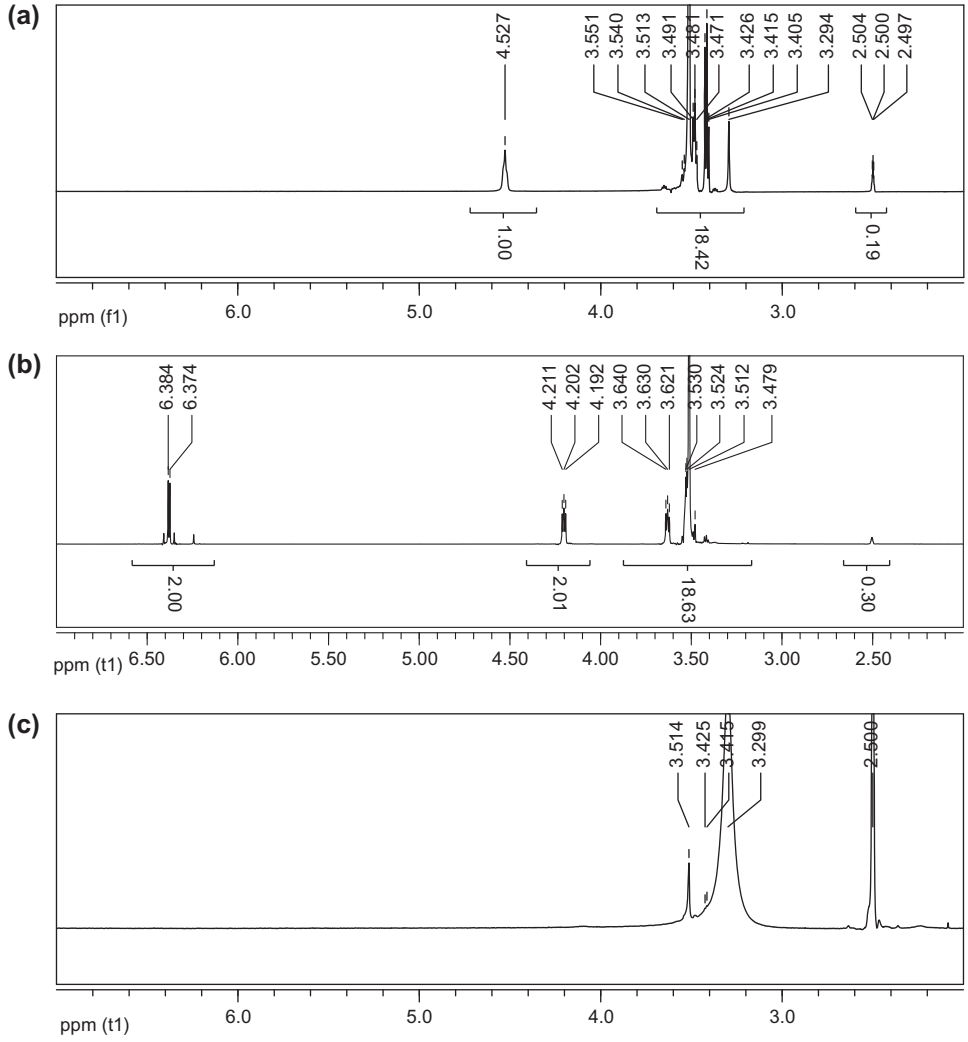

Fig. 4. ^{1}H NMR spectra of PEG (a), PEG_8DMA (b), and PEGDMA-AA (c).

77.6, 89.0, 84.3, and 71.4%, respectively. For PEGDMA-AA (mass ratio 2:5), the inhibition efficiency of $CaCO_3$ scale increases from 12.4 to 67.6% as the dosage increase from 2 to 16 mg/L, being positive correlation relationship and no maximum inhibitory efficiency is observed. What also should be noted is that PEGDMA-AA with mass ratio 1:1 exhibits the best inhibition performance, which is attributed to the appropriate $–OCH_2CH_2/–COOH$ group ratio in the copolymer. When the ratio is higher, the chelating group –COOH is finite, not guaranteeing the combination with a great amount of Ca^{2+} ions, being lower efficiency. Also when the ratio is lower, even though there exists abundant –COOH groups, but the lower content of $–OCH_2CH_2$ (function is to enhance the solubility of polymer-calcium in water) leads the deposition of polymer-calcium particles due to the wretched water solubility of PEGDMA-AA—Ca^{2+} complex. Concluding these, the influence of PEG is significant on scale inhibition which also has been studied in our laboratory before [30].

3.3.2. *Influence of solution property*

As it is known that the inner environment of industrial circulating water system is not invariable throughout, aiding to optimize the parameters of the recycling water process on the industrial scales, investigation of the solution properties effect on PEGDMA-AA inhibition power toward calcium carbonate was carried out. From Fig. 6, we can easily come to a conclusion that inhibition performance on scales is closely related with the solution properties.

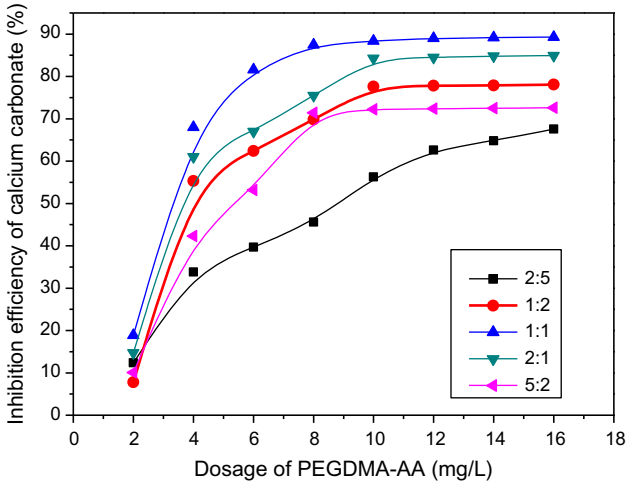

Fig. 5. The influence of dosage and mass ratio (PEGDMA: AA) on $CaCO_3$ inhibition.

In Fig. 6(a), the performance result of PEGDMA-AA using 8 mg/L toward calcium carbonate with a wide variation range of concentration of Ca^{2+} is given out. Surprisingly even in a higher hardness of water condition, PEGDMA-AA still exhibited superior inhibition efficiency exceeding 63.3%, which was rather high to an extent. The reason may be owing to the reaction between Ca^{2+} ions and functional groups –COOH and $–OCH_2CH_2$, resulting the formation of polyion complex (PIC) micelles and the outer PEG chain segments surrounding the core of PIC in water.

Fig. 6(b) demonstrates that when the HCO_3^- concentration (Ca^{2+} keeping at 240 mg/L) is below 720 mg/L, PEGDMA-AA possess unexceptionable calcium carbonate inhibition efficiency, but as the concentration keep increasing to higher concentration, the inhibition efficiency is decreased sharply. Hydrolysis of HCO_3^- produces OH^- and CO_3^{2-} ions which are advantageous to the formation and precipitation of calcium carbonate $CaCO_3$ due to the unceasing pH elevation. Obviously, the influence of alkalinity is enormous.

The higher the temperature is, the more likely the formation of scale, the data in Fig. 6(c) obviously

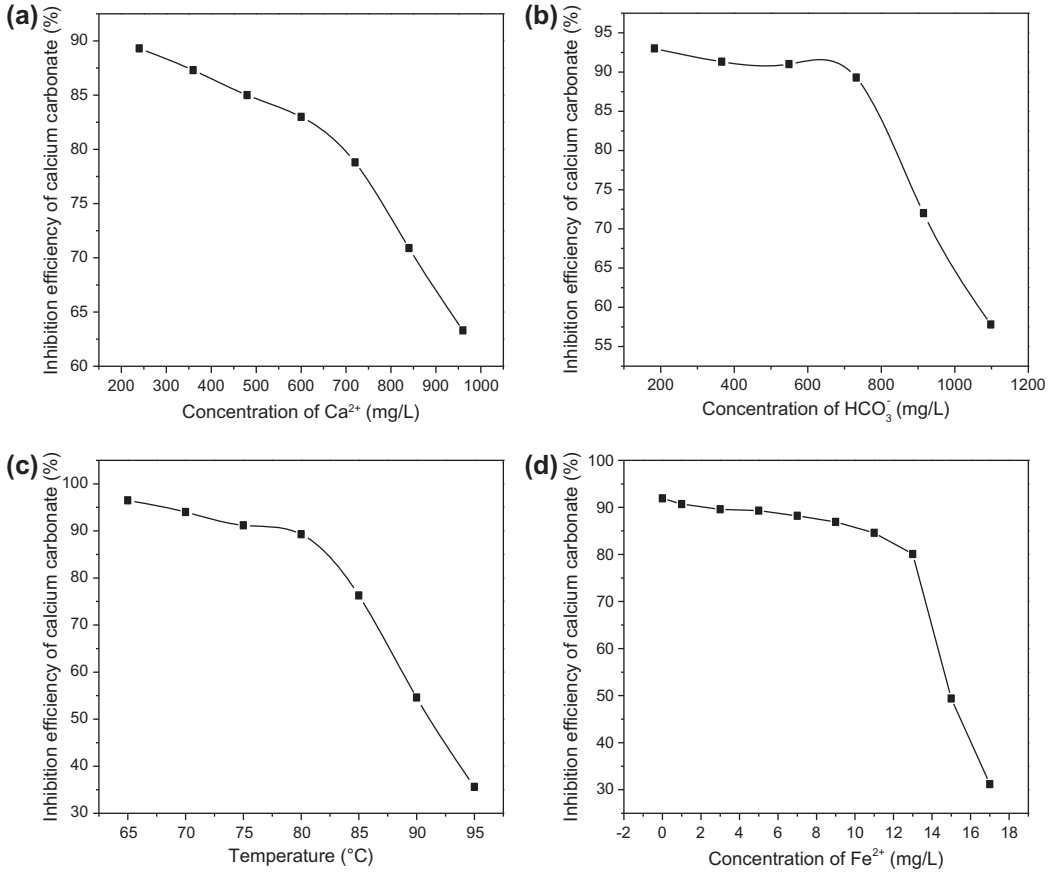

Fig. 6. Inhibition efficiency of calcium carbonate as a function of Ca^{2+} (a), HCO_3^- (b), temperature (c), and Fe^{2+} (d) with 8 mg/L PEGDMA-AA (1:1).

indicates that PEGDMA-AA is a greatly thermal stability polymer, when temperature increases from 65 to 80℃, only 7.4% loss in activity. In industrial practice, the temperature of the warm cooling water returning to cooling towers must be lower than 50℃ to diminish problems caused by scaling. From Fig. 6(c) the inhibition efficiency of calcium carbonate is more than 95% when the temperature is 65℃. Thus, much higher inhibition efficiency will be obtained when the temperature is 50℃. The result indicates that the developed inhibitor can allow higher temperatures for cooling water and, consequently, reduce the consumption of this important resource. Meanwhile, the result also gives the information that higher temperature demands higher concentration to keep the scale maintain ion valence in solution.

As it is well-known that the effectiveness may be lessened for calcium carbonate in the presence of iron ions in solution, so when studying the inhibiting properties, the favorable reaction must be taken into consideration. In Fig. 6(d), we can see that the $CaCO_3$ inhibition efficiency decreased inconspicuously and maintain relatively excellent scale inhibition function until the dosage of Fe^{2+} ions exceed 13 mg/L. From 13 to 17 mg/L, dramatically decreasing is observed. However, the amount of iron ions in industrial water systems are in the order of 1–5 mg/L [26,31], that is to say, PEGDMA-AA still acts as an excellent calcium carbonate inhibitor.

3.3.3. Characterization of $CaCO_3$ scales

Fig. 7 presents the SEM and TEM photographs of calcium carbonate scales. It is obviously that PEGDMA-AA has a great influence on the calcium carbonate crystal morphology and size. Both the morphology and size are greatly varied, the reason is that the modification of a developing crystal is controlled by polymeric through embedding or lattice binding means [32]. In the absence of PEGDMA-AA, the observed crystal display a regular shape of rhombohedra or cubic and the particle size is about 10 μm (Fig. 7(a)). But in the presence of PEGDMA-AA, the regular appearance disappeared and the size dimension decreases to 0.5 ~ 1 μm (Fig. 7(b)). Fracturing into smaller particles (major nucleating sites for scale crystals) in the artificial water accelerate the ejectment of scale deposition. Further research toward $CaCO_3$ crystal was conducted by means of TEM. From Fig. 7(c), integrated symmetrical monoclinic hexahedron calcite crystal appears once more in accordance with SEM image in Fig. 7(a) and a perfect monocrystal pattern is observed. In the presence of PEGDMA-AA, the $CaCO_3$ scale loses its unabridged structure and the asystematic orbicular or circular pattern confirms the destruction of calcite in Fig. 7(d). It is worth mentioned that the lacunose and inner loosened particles have a nanometer order of magnitude diameters modified by PEGDMA-AA, consisted of smaller microcrystal.

The $CaCO_3$ precipitated phases were also indentified by XRD and the corresponding spectra are given out in Fig. 8. In Fig. 8(a), calcite is the only crystal form, the d and θ values conform to the calcite appearing in (012), (104), (006), (110), (113), (202), (018), and (116). And in the presence of PEGDMA-AA, except for the calcite peaks with the same θ angles and decreased intensity, the (004), (110), (112), (114), (300), and (118) peaks corresponding to vaterite also appears (Fig. 8(b)), concluding that calcite and vaterite crystals co-exist with PEGDMA-AA. Meanwhile, obvious differences are discriminated that peaks for calcite at (104), (202), and (116) become weaker accordingly, while (012), (006), (110), 113), and (018) peaks are weak to disappear in the spectra Fig. 8(b). Above all, the crystal forms are altered in addition to the crystallographic degree to an extent.

The crystal transformations were also investigated by means of FTIR. In the Fig. 9(a) there are only calcite absorption peaks in 872 and 710 cm^{-1} [33]. Upon the addition of PEGDMA-AA, new 741 cm^{-1} peaks emerged which further prove the calcite-vaterite transformation as depicted in Fig. 9(b). The SEM, TEM, XRD, and FTIR results strongly manifests the great influence of PEGDMA-AA to the crystal size, shape, and crystal form.

3.4. Dispersion test for Fe(III)

3.4.1. The influence of dosage and mass ratio (PEGDMA: AA) on dispersion for Fe(III)

The influence of dosage and mass ratio (PEGDMA: AA) on dispersion for Fe(III) is presented in Fig. 10. The relation between dosage of PEGDMA-AA and transmittance is negative correlation ahead of the polymeric threshold dosage value, that is to say, as the dosage goes up, the dispersion capacity for Fe(III) becomes bigger and bigger until a constant value. The smaller the transmittance is, the more excellent the dispersion power is. The threshold value for PEGDMA-AA (mass ratio 2:5), PEGDMA-AA (mass ratio 1:2), PEGDMA-AA (mass ratio 1:1), PEGDMA-AA (mass ratio 2:1), PEGDMA-AA (mass ratio 5:2) is 12, 6, 6, 8, 10 mg/L, respectively, and the corresponding minimum light transmittance is 22.0, 17.1, 19.7, 21.6, 24.7. Mass ratio 1:2 is the best reaction ratio for dispersing Fe(III), while the best ratio for inhibition $CaCO_3$ is 1:1. The difference may be due to the

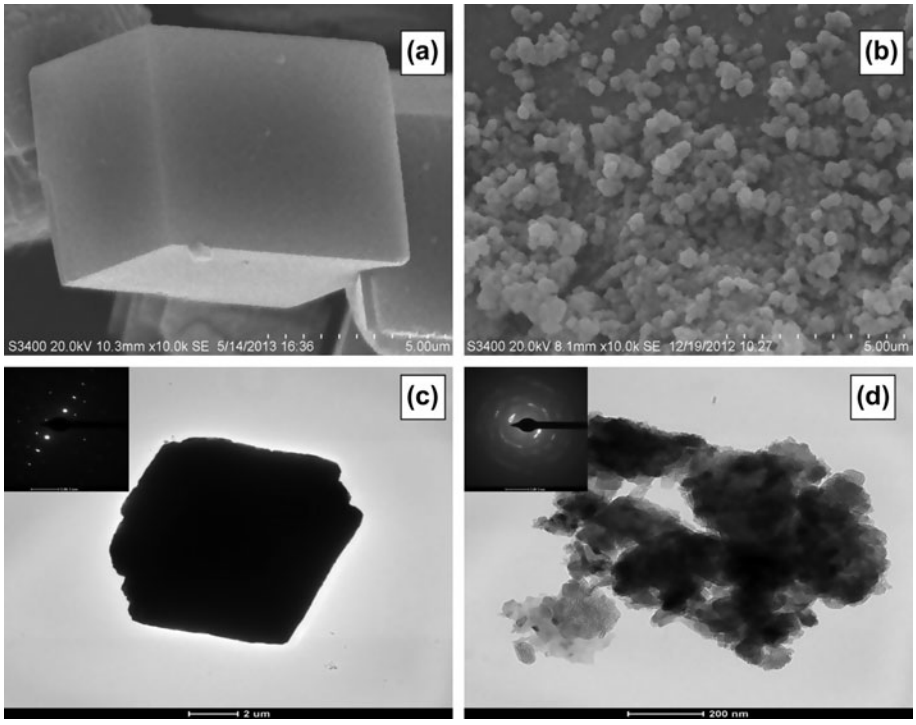

Fig. 7. The SEM and TEM photographs of $CaCO_3$ without inhibitor (a) and (c) and with 8 mg/L PEGDMA-AA (b) and (d) (PEGDMA: AA = 1:1).

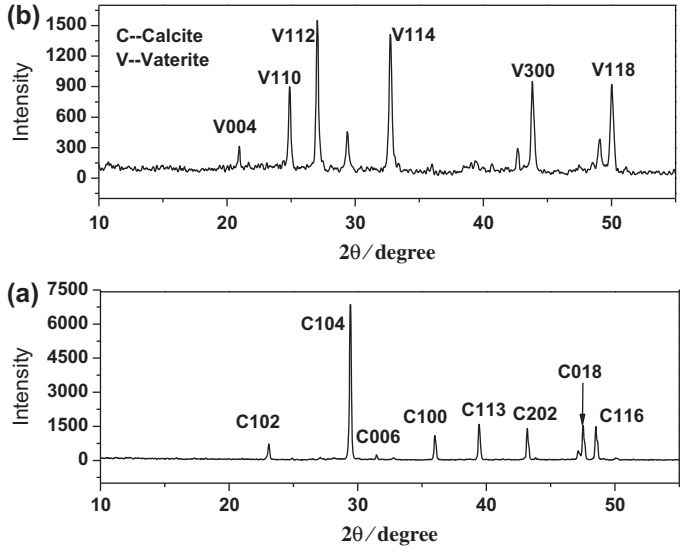

Fig. 8. The XRD pattern of $CaCO_3$ without inhibitor (a) and in the presence of 8 mg/L PEGDMAAA (b) (PEGDMA: AA = 1:1).

discriminative need for the $–OCH_2CH_2–$/–COOH proportion in the PEGDMA-AA structure. In other words, the appropriate molecule weight is different for the $CaCO_3$ and Fe scales inhibition. The fundamental impetus of inhibition is supposed to arise from the interactions between iron ions with –COOH groups located at the side chains of PEGDMA-AA. –COOH groups are capable of recognizing and encapsulating positively charged iron ions (Fe^{2+} or Fe^{3+}) thus forming complex micelles. The higher the molecule weight

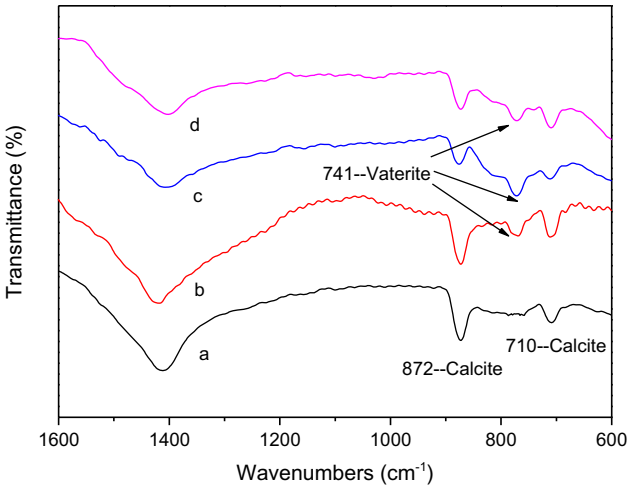

Fig. 9. The FTIR spectra of $CaCO_3$ scales without inhibitor (a) and with of 2 mg/L (b), 4 mg/L (c), 8 mg/L (d) PEGDMA-AA (PEGDMA: AA = 1:1).

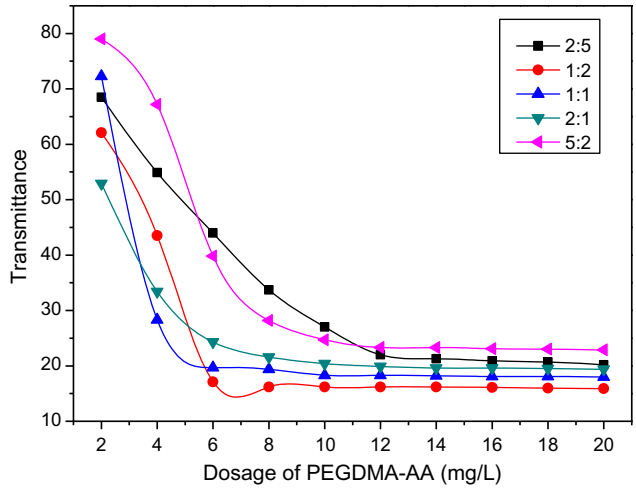

Fig. 10. The influence of dosage and mass ratio (PEGDMA: AA) on dispersion for Fe(III).

is, the longer the molecule chain. After the adsorption or bonding with Fe^{3+} ions, the larger complex micelles are easy to settle down. And while the molecule weight is too low, the density of chelating charge is not sufficient thus exhibit poor dispersion performance. The PEG segments surround the complex micelles surface and act the function of improving dissolvability (Fig. 11).

3.4.2. Comparison with commercial inhibitors

Table 1 lists the comparison result of PEGDMA-AA, PAA, PESA, HPMA, PBTC, and HEDP in the dispersion for Fe(III), and obviously the latter inhibitors show approximately no dispersion ability when PEGDMA-AA demonstrate superior dispersion power, contrarily only 6 mg/L dosage to get the transmittance below 20. These inhibitors contain carboxyl groups, hydroxyl, and/or phosphonic acid functional groups in their molecular structures that own strong affinity to multivalent cations, such as Ca^{2+}, Fe^{2+} and the like [34]. Analyzing the data for iron scale and the structures of the used inhibitors, it is easy to end the conclusion that double hydrophilic block copolymer PEGDMA-AA is more excellent than inhibitors which only have one hydrophilic function group in dispersing Fe(III), which is due to the water-soluble PEG in the matrix of PEGDMA-AA [30].

3.5. Mechanism of PEGDMA-AA on scale inhibition and dispersion

The calcium scale deposition from the saturation solution obey the following two process: crystal nucleus generation and crystal nucleus growth into crystals [35], while the Fe scale form and deposit immediately upon the collision between Fe^{2+}, Fe^{3+} and OH^-, SO_4^{2-}, CO_3^{2-}. PEGDMA-AA molecules possess

Table 1
Transmittance of solution of different inhibitors

Dosage of scale inhibitors (mg/L)	Transmittance of solution					
	PEGDMA-AA	PAA	PESA	HPMA	PBTC	HEDP
2	72.3	96.0	95.3	97.0	93.1	94.3
4	28.3	96.6	88.7	95.4	94.5	93.9
6	19.7	96.2	79.5	97.3	92.4	90.0
8	19.4	95.8	90.5	95.5	92.4	88.5
10	18.3	95.4	97.1	97.1	90.3	74.0
12	18.3	96.8	94.3	97.0	83.1	77.0
14	18.2	96.6	94.7	97.1	88.9	75.3
16	18.1	96.3	96.6	97.0	81.4	65.4

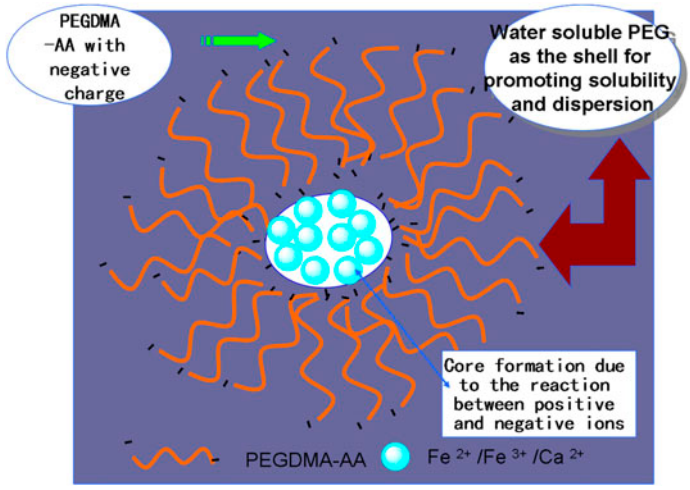

Fig. 11. Scale inhibition and dispersion mechanism of PEGDMA-AA.

strong chelating capacity after ionizing into anionic polymer due to the physical or chemical effect. Both PEGDMA and AA contain –COOH groups, guaranteeing the strong chelating power. Once confronted with Ca^{2+}, Fe^{2+}, or Fe^{3+} ions, –COOH immediately reacts or bonds with them but not on the basis of stoichiometric ratio, and the most part of oxygen atoms are shared between calcium ions or ferric ions [36]. The spontaneous produced PEGDMA-AA-Ca or PEGDMA-AA-Fe result in the core formation. Meanwhile, water compatible PEG segments surround the core and serve as the shell. The PEGDMA-AA-Ca^{2+} or PEGDMA-AA-Fe^{3+} solubility is enhanced by forming hydrogen bonds, thus the depositon process of scales is prevented. Such suspended solids are not easy to settle down, not to speak of the mutual collision and aggregation into larger particle, thereby dispersing and washing out them throughout a fluid [37].

4. Conclusions

Double hydrophilic PEG-based block polymer PEGDMA-AA was synthesized and confirmed by FTIR and ^{1}HNMR in this study. The static jar scale inhibition test exhibited that the maximum calcium carbonate inhibition efficiency is 89.0% using 8 mg/L PEGDMA-AA (mass ratio 1:1). Investigation of influence of solution properties on $CaCO_3$ inhibition gave the fact that PEGDMA-AA maintains most of their activity with the calcium hardness of 240–720 mg/L, alkalinity of 183–795 mg/L, temperature of 65–85°C, and at levels of 1–13 mg/L iron ions in aqueous solutions. SEM and TEM indicated that both the crystal morphology and size took great place upon the addition of PEGDMA-AA. XRD and FTIR manifested the crystal form transfer. The optimal ratio was 1:2 for Fe(III) dispersion test with minimum transmittance 19.7 using 6 mg/L PEGDMA-AA and comparison with commercial inhibitors concluded that double hydrophilic polymer is better than water treatment agents, which have only one double hydrophilic chelating group (such PAA and HPMA). The inhibition mechanism toward $CaCO_3$ and iron scales is supposed to be the formation of PEGDMA-AA-Ca^{2+} and PEGDMA-AA-Fe^{3+}, while the PEG segments enhance the solubility of chelating complex.

Acknowledgments

This work was supported by the Prospective Joint Research Project of Jiangsu Province [BY2012196]; the National Natural Science Foundation of China [51077013]; Special funds for Jiangsu Province Scientific and Technological Achievements Projects of China [BA2011086]; Program for Training of 333 High-Level Talent, Jiangsu Province of China [BRA2010033]; Scientific Innovation Research Foundation of College Graduate in Jiangsu Province (CXLX13-107).

References

[1] E. Rubio-Castro, M. Serna-González, J.M. Ponce-Ortega, M.M. El-Halwagi, Synthesis of cooling water systems with multiple cooling towers, Appl. Therm. Eng. 50 (2013) 957–974.
[2] E. Rubio-Castro, M. Serna-González, J.M. Ponce-Ortega, Optimal design of effluent-cooling systems using a mathematical programming model, Appl. Therm. Eng. 30 (2010) 2116–2126.
[3] J.M. Ponce-Ortega, M. Serna-González, A. Jiménez-Gutiérrez, Optimization model for re-circulating

cooling water systems, Comput. Chem. Eng. 34 (2010) 177–195.
[4] J.M. Ponce-Ortega, M. Serna-González, A. Jiménez-Gutiérrez, A disjunctive programming model for simultaneous synthesis and detailed design of cooling networks, Chem. Eng. 48 (2009) 2991–3003.
[5] J.-K. Kim, R. Smith, Cooling water system design, Chem. Eng. Sci. 56 (2001) 3641–3658.
[6] G.F. Cortinovis, M.T. Ribeiro, J.L. Paiva, T.W. Song, Integrated analysis of cooling water systems: Modeling and experimental validation, Appl. Therm. Eng. 29 (2009) 3124–3131.
[7] F. Liu, X.H. Lu, W. Yang, J.J. Lu, H.Y. Zhong, X. Chang, C.C. Zhao, Optimizations of inhibitors compounding and applied conditions in simulated circulating cooling water system, Desalination 313 (2013) 18–27.
[8] M.T.G. Ruelo, L.D. Tijing, A. Amarjargal, C.-H. Park, H.J. Kim, H.R. Pant, D.H. Lee, C.S. Kim, Assessing the effect of catalytic materials on the scaling of carbon steel, Desalination 313 (2013) 189–198.
[9] A. Tsortos, G.H. Nancollas, The role of polycarboxylic acids in calcium phosphate mineralization, J. Colloid Interface Sci. 250 (2002) 159–167.
[10] Y.M. Tang, W.Z. Yang, X.S. Yin, Y. Liu, P.W. Yin, J.T. Wang, Investigation of $CaCO_3$ scale inhibition by PAA, ATMP and PAPEMP, Desalination 228 (2008) 55–60.
[11] H.K. Moudgil, S. Yadav, R.S. Chaudhary, Synergistic effect of some antiscalants as corrosion inhibitor for industrial cooling water system, J. Appl. Electrochem. 39 (2009) 1339–1347.
[12] A.G. Xyla, J. Mikroyannidis, P.G. Koutsoukos, The inhibition of calcium carbonate precipitation in aqueous media by organophosphorus compounds, J. Colloid Interface Sci. 153 (1992) 537–551.
[13] C.E. Fu, Y.M. Zhou, G.Q. Liu, J.Y. Huang, W.D. Wu, W. Sun, Carboxylate-ended poly(ethylene glycol) macromonomers and their copolymers as inhibitors for calcium phosphate and calcium sulfate, Int. J. Polym. Mater. 61 (2012) 341–356.
[14] S.G. Rees, D.T.H. Wassell, R.P. Shellis, G. Embery, Effect of serum albumin on glycosaminoglycan inhibition of hydroxyapatite formation, Biomaterials 25 (2004) 971–977.
[15] A.A. Koelmans, A. Van der Heijde, L.M. Knijff, R.H. Aalderink, Integrated modelling of eutrophication and organic contaminant fate & effects in aquatic ecosystems. A review, Water. Res. 35 (2001) 3517–3536.
[16] D. Hasson, G. Sidorenko, R. Semiat, Calcium carbonate hardness removal by a novel electrochemical seeds system, Desalination 263 (2010) 285–289.
[17] T. Kumar, S. Vishwanatham, S.S. Kundu, A laboratory study on pteroyl-L-glutamic acid as a scale prevention inhibitor of calcium carbonate in aqueous solution of synthetic produced water, J. Petrol. Sci. Eng. 71 (2010) 1–7.
[18] P. Shakkthivel, T. Vasudevan, Acrylic acid-diphenylamine sulphonic acid copolymer threshold inhibitor for sulphate and carbonate scales in cooling water systems, Desalination 197 (2006) 179–189.
[19] C. Wang, S.P. Li, T.D. Li, Calcium carbonate inhibition by a phosphonate-terminated poly(maleic-co-sulfonate) polymeric inhibitor, Desalination 249 (2009) 1–4.
[20] D. Kralj, L. Brečević, J. Kontrec, Vaterite growth and dissolution in aqueous solution III: Kinetics of transformation, J. Cryst. Growth. 177 (1997) 248–257.
[21] G.Q. Liu, Y.M. Zhou, J.Y. Huang, Q.Z. Yao, L. Ling, P.X. Zhang, X.F. Zhong, C.E. Fu, W.D. Wu, W. Sun, Carboxylate-terminated double-hydrophilic block copolymer as an effective and environmentally friendly inhibitor for carbonate and sulfate scales in cooling water systems, Water Air Soil Poll. 223 (2012) 3601–3609.
[22] F. Wurm, H. Frey, Linear-dendritic block copolymers: The state of the art and exciting perspectives, Prog. Polym. Sci. 36 (2011) 1–52.
[23] E. Dalas, P. Klepetsanis, P.G. Koutsoukos, The overgrowth of calcium carbonate on poly(vinyl chloride-co-vinyl acetate-co-maleic acid), Langmuir 15 (1999) 8322–8327.
[24] J. Guo, S.J. Severtson, Application of classical nucleation theory to characterize the influence of carboxylate-containing additives on $CaCO_3$ nucleation at high temperature, pH, and ionic strength, Ind. Eng. Chem. Res. 42 (2003) 3480–3486.
[25] J.D. Zhang, L. Chen, H.M. Zeng, X.X. Yan, X.N. Song, H. Yang, C.S. Ye, Pilot testing of outside-in MF and UF modules used for cooling tower blowdown pretreatment of power plants, Desalination 214 (2007) 287–298.
[26] C.E. Fu, Y.M. Zhou, J.Y. Huang, H.T. Xie, G.Q. Liu, W.D. Wu, Control of iron(III) scaling in industrial cooling water systems by the use of maleic anhydride-ammonium allylpolyethoxy sulphate dispersant, Adsorpt. Sci. Technol. 28 (2010) 437–448.
[27] A.A.-D. Muna, A.F.A.-R. Nathir, A. Ayman, Evaluating the performance of sulfonated kraft lignin agent as corrosion inhibitor for iron-based materials in water distribution systems, Desalination 313 (2013) 105–114.
[28] X. Zhao, X.D. Chen, A critical review of basic crystallography to salt crystallization fouling in heat exchangers, Heat Trans. Eng. 34 (2013) 719–732.
[29] H. Cölfen, Double-hydrophilic block copolymers: Synthesis and application as novel surfactants and crystal growth modifiers, Macromol. Rapid. Commun. 22 (2001) 219–252.
[30] G.Q. Liu, J.Y. Huang, Y.M. Zhou, Q.Z. Yao, L. Ling, P. Zhang, C.E. Fu, W.D. Wu, W. Sun, Acrylic acid-allylpolyethoxy carboxylate copolymer dispersant for calcium carbonate and iron(III) hydroxide scales in cooling water systems, Tenside Surfact. Det. 49 (2012) 216–224.
[31] C.E. Fu, Y.M. Zhou, H.T. Xie, W. Sun, W.D. Wu, Double-hydrophilic block copolymers as precipitation inhibitors for calcium phosphate and iron (III), Ind. Eng. Chem. Res. 49 (2010) 8920–8926.
[32] H. Cölfen, M. Antonietti, Crystal design of calcium carbonate microparticles using double-hydrophilic block copolymers, Langmuir 14 (1998) 582–589.
[33] H.R. Yang, Y.N. Su, H.J. Zhu, H. Zhu, B.Q. Xie, Y. Zhao, Y.M. Chen, D.J. Wang, Synthesis of amphiphilic triblock copolymers and application for morphology

control of calcium carbonate crystals, Polymer 48 (2007) 4344–4351.
[34] J.J. Xie, X.R. Liu, J.F. Liang, Y.S. Luo, Swelling properties of superabsorbent poly(acrylic acid-co-acrylamide) with different crosslinkers, J. Appl. Polym. Sci. 112 (2009) 602–608.
[35] D. Liu, F. Hui, J. Lédion, F.T. Li, Study of the scaling formation mechanism in recycling water, Environ. Tech. 32 (2011) 1017–1030.
[36] A. Harada, K. Kataoka, Formation of polyion complex micelles in an aqueous milieu from a pair of oppositely-charged block copolymers with poly(ethylene glycol) segments, Macromolecules 28 (1995) 5294–5299.
[37] W. Tjandra, J. Yao, P. Ravi, K.C. Tam, A. Alamsjah, Nanotemplating of calcium phosphate using a double-hydrophilic block copolymer, Chem. Mater. 17 (2005) 4865–4872.